Carbohydrate Polymers 88 (2012) 1100–1108

Contents lists available at SciVerse ScienceDirect

Carbohydrate Polymers

journal homepage: www.elsevier.com/locate/carbpol

Alginate/graphene oxide fibers with enhanced mechanical strength prepared by wet spinning

Yongqiang He[a,b], Nana Zhang[b], Qiaojuan Gong[a], Haixia Qiu[b,*], Wei Wang[b], Yu Liu[b], Jianping Gao[b,*]

[a] Department of Applied Chemistry, Yuncheng University, Yuncheng 044000, PR China
[b] School of Science, Tianjin University, Tianjin 300072, PR China

ARTICLE INFO

Article history:
Received 9 December 2011
Received in revised form 9 January 2012
Accepted 23 January 2012
Available online 1 February 2012

Keywords:
Alginate
Graphene oxide
Composite fiber
Mechanical strength
Cells culture

ABSTRACT

Sodium alginate/graphene oxide (NaAlg/GO) fibers were prepared using a wet spinning method. Their structures and properties were characterized by Fourier transform infrared spectroscopy, scanning electron microscopy, X-ray diffraction and mechanical strength testing. The incorporation of GO significantly improved the strength of the NaAlg/GO fibers owing to the uniform distribution of the GO nanosheets in the NaAlg matrix. The maximum tensile strength and Young's modulus increased from 0.32 and 1.9 to 0.62 and 4.3 GPa, respectively, at 4 wt% GO loading. The composite fibers had an even higher strength when they were stretched. The tensile strength increased by 43% over the un-stretched fiber, and Young's modulus increased to 9.39 GPa. In aqueous solution, the GO/NaAlg fibers swelled to form hydrogel fibers that are nontoxic to cells which demonstrated the potential applications of the as-spun fibers in wound dressing materials.

1. Introduction

Alginate (NaAlg) is a natural polysaccharide extracted from brown seaweeds. Since it was discovered, alginate has been used in a wide range of industries, such as textile printing, paper (Khan, Huq, Saha, Khan, & Khan, 2010). As its some unique properties such as non-toxicity, hydrophilicity, biocompatibility and a relatively low cost (Chung et al., 2002; Sennerby, Rostlund, Albrektsson, & Albrektsson, 1987), alginate has been widely used in the wound management industry as a novel material for the manufacture of 'moist healing' products such as gels, foams and fibrous non-woven dressings that are used to cover wounds (Balakrishnan, Mohanty, Umashankar, & Jayakrishnan, 2005; Khan et al., 2010). Alginate is water-soluble and can form hydrogels in the presence of divalent cations (like Ca^{2+} (Woraharn, Chaiyasut, Sirithunyalug, & Sirithunyalug, 2010)), due to ionic cross-linking via calcium bridges between the L-guluronic acid residues on adjacent chains. Because of its reversible solubility, alginate can be fabricated in various forms, such as films, microspheres and fibers (Bogun, Mikolajczyk, & Rabiej, 2009; Dong, Wang, & Du, 2006; Watthanaphanit, Supaphol, Tamura, Tokura, & Rujiravanit, 2010). Over the last two decades, alginate fibers have become well established in the wound treatment industry (Qin, 2008; Qin, Hu, & Luo, 2006) where their ion-exchange and gel-forming abilities are particularly useful for the treatment of exuding wounds. Despite this, alginate fibers themselves still display some unsatisfactory properties such as low mechanical strength. Many modifications have been made to improve their properties, for example, sodium alginate (NaAlg) blends or spinning with a non-toxic polymer such as gelatin (Choi et al., 1999), chitosan (CS) (Wang et al., 2010), or poly(ethylene oxide) (Lu, Zhu, Guo, Hu, & Yu, 2006).

Modification of polymers with inorganic materials is another way to improve polymer properties such as mechanical strength (Coleman, Khan, Blau, & Gun'ko, 2006; Han, Yan, Chen, Li, & Bangal, 2011) and thermal conductivity (Huang, Liu, Wu, & Fan, 2005). For example, Chatterjee, Lee, and Woo (2009) prepared CS/carbon nanotube (CNT) hydrogel beads, and the force needed to cause complete breakdown of the CS hydrogel beads increased from 1.87 to 7.62 N owing to the incorporation of the carbon nanotubes (CNTs). Sa and Kornev (2009) fabricated NaAlg/single-walled carbon nanotube (SWCNT) fibers that had a maximum Young's modulus of 6.38 GPa at 23 wt SWCNT loading. Recently, graphene/graphene oxide (GO) as a star in materials research has been attracting tremendous attentions in the past few years in various fields including biomedicine (Feng, Zhang, & Liu, 2011; Li & Kaner, 2008; Li, Liu, & Ma, 2011). GO has a large theoretical specific surface area and a large number of functional groups, such as —OH, —COOH, —O—, and C=O which make GO hydrophilic, readily dispersible in water as well as other solvents, and easily modified to be compatible with polymer matrixes (Meyer et al., 2007). Since GO is prepared from low-cost graphite, it has an outstanding price advantage over CNTs, and this has encouraged studies of GO/synthetic polymer

* Corresponding authors. Tel.: +86 22 274 041 18; fax: +86 22 274 034 75.
E-mail addresses: qhx@tju.edu.cn (H. Qiu), jianpingg@eyou.com (J. Gao).

0144-8617/$ – see front matter © 2012 Elsevier Ltd. All rights reserved.
doi:10.1016/j.carbpol.2012.01.071

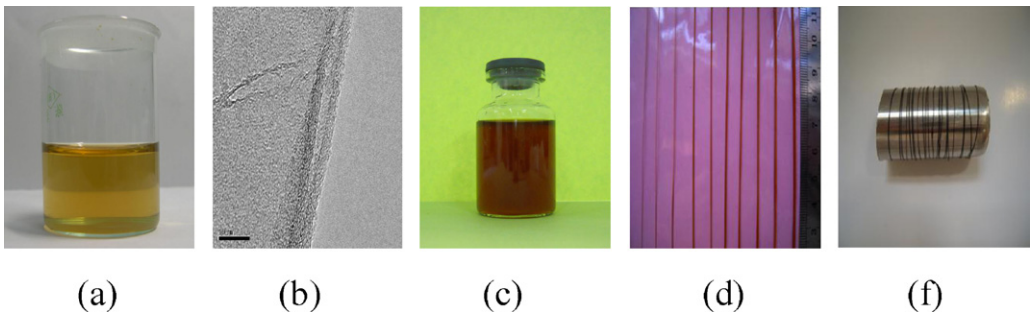

Fig. 1. Photo of GO suspension (a), TEM photo of GO nanosheets (b), spinning solution (c), gel fibers with different diameters (d), and dry fibers (f).

composites (Celzard et al., 1996; Chen, Muller, Gilmore, Wallace, & Li, 2008; Dikin et al., 2007; Paci, Belytschko, & Schatz, 2007; Stankovich et al., 2006). GO has also been used to reinforce natural polymers such as CS films and CS-gelatin porous monoliths (Zhang et al., 2006).

As far as we know, no studies on the usage of GO nanosheets in NaAlg have been reported. In this study, NaAlg/GO fibers were fabricated by a wet spinning method and their structure and properties were characterized.

2. Materials and methods

2.1. Materials

Graphite was from Huadong Graphite Factory, NaAlg was from Catalogue of Fine Chemicals. All other reagents were analytical grade and from Tianjin Chemical Reagent Co. All chemicals were used as received.

2.2. Preparation of GO

GO was prepared from purified natural graphite by a modified Hummer's method (Hummers & Offeman, 1958). Briefly, concentrated H_2SO_4 was added into a 250 mL flask filled with graphite, followed by the addition of $NaNO_3$, and then solid $KMnO_4$ was gradually added with stirring. The mixture was kept below 20 °C and stirred with a mechanical stir bar for 2 h. Excess distilled water was added into the mixture and then the temperature was increased to and maintained at 35 °C for half an hour. The temperature was then increased to 90 °C and the mixture was stirred for another 0.5 h. Finally 30% H_2O_2 was added until the color of mixture changed to brilliant yellow and there was no gas being produced. The mixture was filtered and washed three times with 5% aqueous HCl to remove metal ions and then washed with distilled water to remove the acid. The resulting filter cake was dried in air and dispersed into water. Suspended GO nanosheets were obtained after ultrasonic treatment for 3 h. Transmission electron microscopy (TEM) measurements were performed using a Philips Tecnai G2F20 microscope at 200 kV.

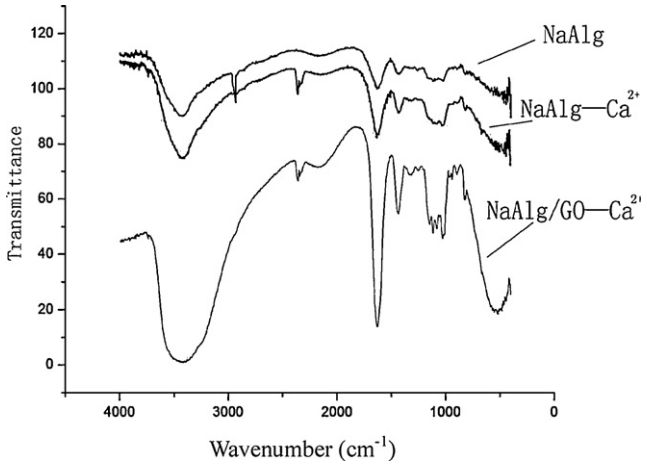

Fig. 2. FT-IR spectra of the NaAlg fibers and GO/NaAlg fibers.

2.3. Preparation of NaAlg/GO fibers

NaAlg/GO fibers were prepared using a wet spinning method (Speakman & Chamberlain, 1944), in which a calcium chloride solution was used as a coagulation bath. Briefly, GO aqueous suspensions with different concentrations were prepared by ultrasonic treatment, and then a certain volume of NaAlg solution was added and the resulting solution was stirred constantly for about 3 h to form a series of NaAlg/GO solutions with different NaAlg/GO ratios. Each solution was squeezed through a needle and drawn into the coagulation bath at room temperature. The spun fibers were collected and soaked in pure water for 10 min, and were then rinsed several times and dried to a constant weight.

To obtain composite fibers with different draw ratios, the cured gel fibers were drawn to a certain length before they were again put into the coagulation bath to cure for several minutes, and then they were rinsed several times and dried to a constant weight.

2.4. Fourier transform infrared (FT-IR) spectra analysis of NaAlg/GO fibers

The FT-IR spectra of NaAlg/GO were measured with a BIO-BAD FTS3000 FT-IR spectrometer in the wavelength range of 500–4000 cm^{-1}.

2.5. Scanning electron microscopy (SEM) analysis of NaAlg/GO fibers

The morphology of the NaAlg/GO fibers was observed by SEM (JEOL-6700F ESEM, Japan). The samples were first coated with gold using a sputter coater (Desk-II; Denton Vacuum) and then placed onto the stage in the chamber for observation.

2.6. Mechanical properties of NaAlg/GO fibers

Fibers with uniform diameters were cut into short pieces of about 4 cm in length, and then they were put into a humidity control chamber for 24 h (relative humidity = 45%). Tensile strength and elongation at the break of the fibers were measured by a mechanical tester (Testometric M-350KN) at a strain rate of 5 mm/min. The tensile strength (δ) was calculated with the following formula:

$$\delta = \frac{F}{A}$$

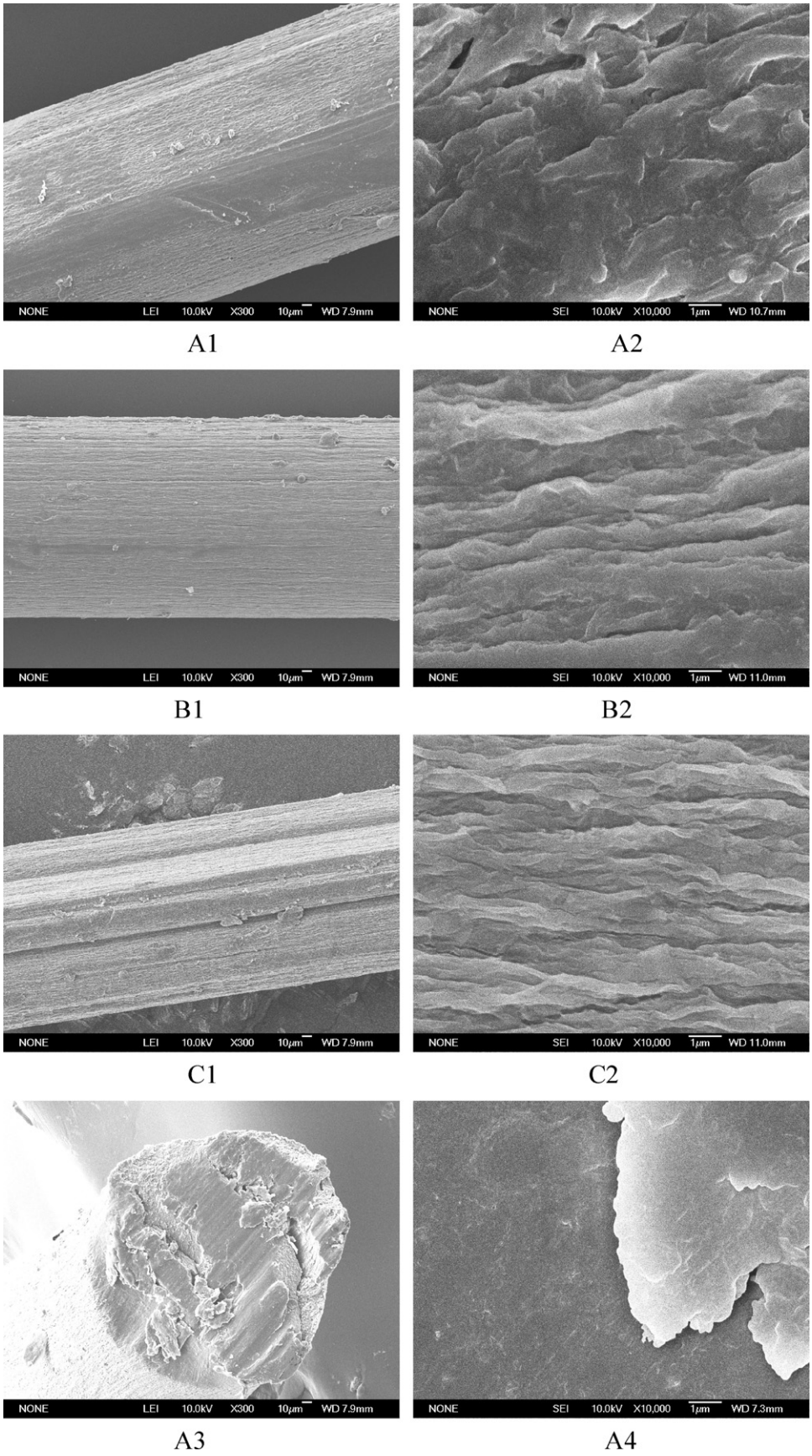

Fig. 3. SEM images of GO/NaAlg fibers with different GO contents (A) 0 wt%; (B) 4 wt%; (C) 8 wt%.

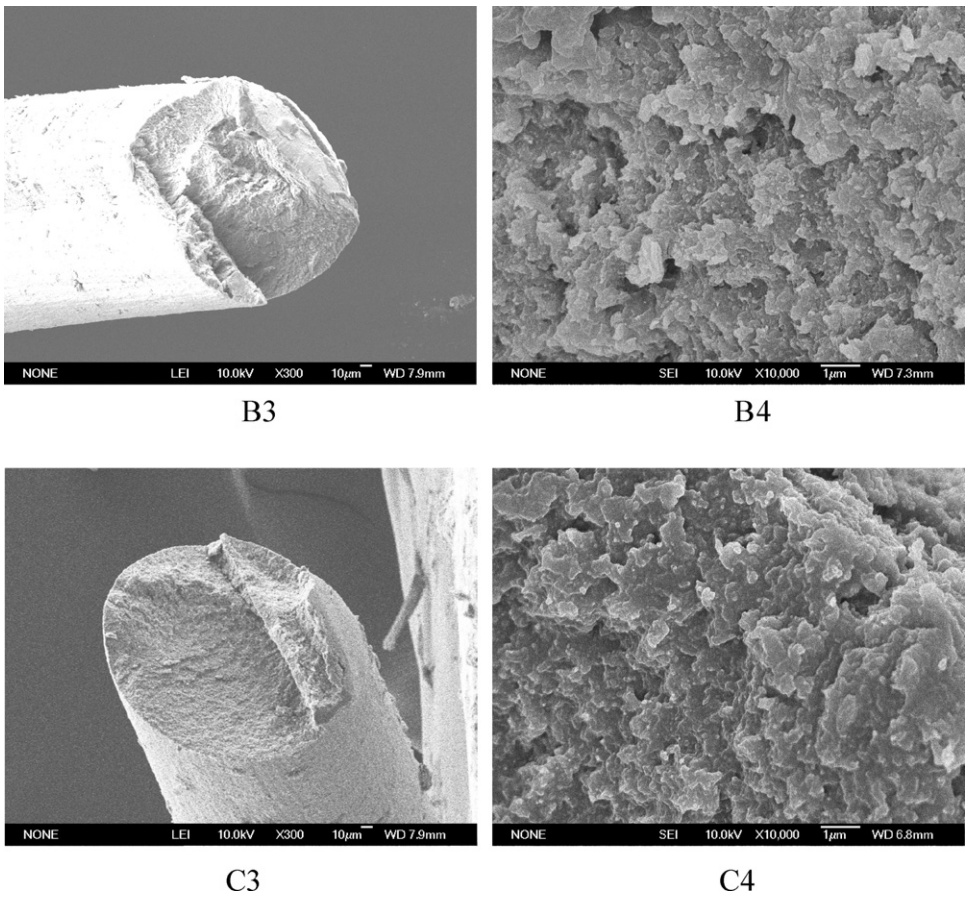

Fig. 3. (*Continued*).

where F is the maximum force and A is the cross-sectional area of the fibers. For each kind of fiber, the data is the mean value of at least three independent measurements.

2.7. Water absorbency of NaAlg/GO fibers

For the water absorbency analysis, the fibers were first placed into a vacuum at 50 °C to dry to a constant weight, and then they were immersed in water or other solution. After soaking for 1 h at room temperature, the samples were removed and blotted with filter paper before being weighed. The water absorption of NaAlg/GO fibers was calculated according to the following equation:

$$\text{Water absorbency} \quad (\text{g/g}) = \frac{W_t - W_o}{W_o}$$

where W_o and W_t (g) are the weight of NaAlg/GO fibers before and after immersion into water, respectively. All the final data is the mean value of three independent measurements.

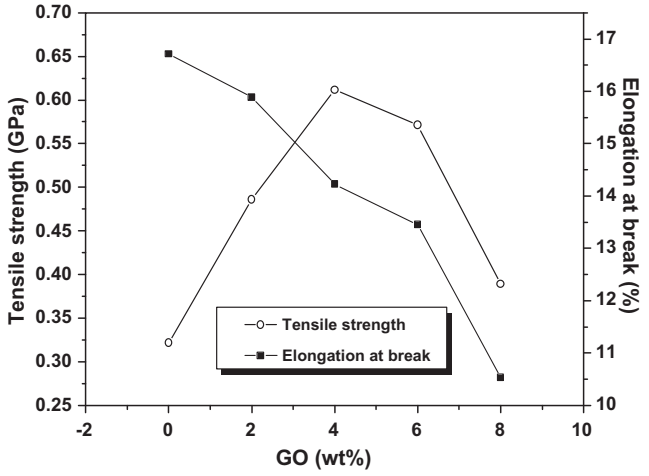

Fig. 4. Tensile strength and elongation at the breake of GO/NaAlg fibers with different GO loadings.

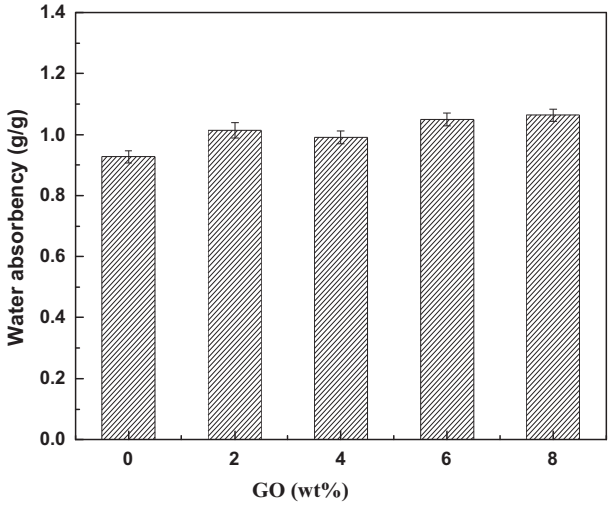

Fig. 5. Effects of GO concentrations on the water absorbency of the GO/NaAlg fibers (4 wt% GO).

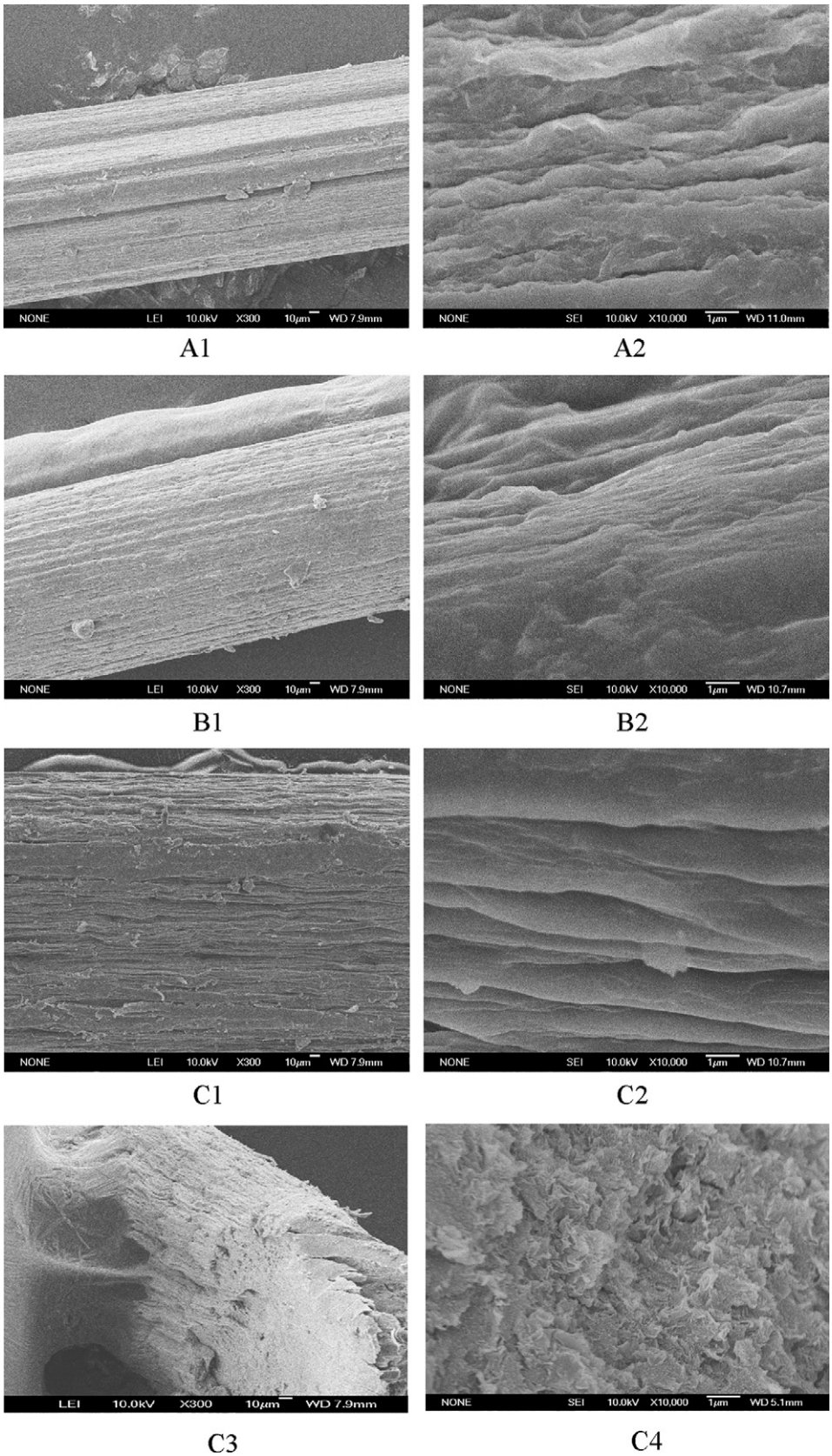

Fig. 6. SEM images of GO/NaAlg fibers with different draw ratios. (A1, A2) 0%; (B1, B2) 50%; (C1, C2, C3, C4) 100%.

2.8. In vitro cell culture and cell morphology

Frozen rabbit transparent cartilage cells obtained from rabbit original articular cartilage (Wu, Wan, Cao, & Wu, 2008) were first recovered and cultured at 37–39 °C. After the cells' fifth passage, they were used as model cells to be seeded onto the GO/NaAlg fibers. The composite fibers were thoroughly washed to remove any free calcium chloride and disinfected by γ-ray radiation for 24 h before cell culturing. The treated composite fibers were placed on round glass coverslips, put into 6-well culture plates and incubated with 2 mL Dulbecco's modified Eagle's medium (DMEM) for 30 min at 37 °C under a 95% air/5% CO_2 atmosphere. Then the DMEM medium was discarded, and 2 mL of DMEM containing rabbit's transparent cartilage cells was inoculated onto the composite fibers and around the bare cells as a control. The samples were then cultured in DMEM (Gibco) buffered with N-(2-hydroxyethyl) piperazine-N′-2-ethanesulfonic acid (HEPES). The cell culture was maintained in a rotational gas jacket incubator with a 5% CO_2 atmosphere at 37 °C for 1 week. Cell growth was observed every day, and the media were changed every 3 days.

3. Results and discussion

3.1. GO and NaAlg/GO fibers

The GO used for preparing the NaAlg/GO fibers was synthesized in our lab. The exfoliated GO can be readily dispersed in water with mild ultrasonic treatment and forms a transparent suspension that is stable for several months with no precipitation (Fig. 1(a)). TEM demonstrated that the GO nanosheets consist of one to several layers (Fig. 1(b)), so they are stably dispersed in water and organic solvents. NaAlg and GO both contain negative ions, which causes electrostatic repulsions between NaAlg and GO, and allow GO to be well dispersed in a NaAlg aqueous solution so that a uniform spinning solution is formed (Fig. 1(c)). After the spinning solution was extruded through the orifice of the needle, gel-state fibers were formed on contact with the coagulation solution. The fiber diameters depend on the inner diameter of the needle (Fig. 1(d)). After remaining in air for several days, dried fibers were obtained. The fibers look smooth and have uniform diameters (Fig. 1(f)).

3.2. FT-IR spectra of the NaAlg fiber and NaAlg/GO fibers

FT-IR spectra of the NaAlg fiber and NaAlg/GO fiber are shown in Fig. 2. The NaAlg–Ca^{2+} fiber has a similar IR spectrum to that of the NaAlg fiber except for the absorption peak at 2938 cm^{-1} which can be assigned to the NaAlg C–H asymmetric stretching vibration. This peak is weak in the NaAlg–Ca^{2+} fiber because of the cross-linkage of NaAlg with Ca^{2+}. The NaAlg macromolecules and Ca^{2+} ions form an "egg-box" structure that limits C–H stretching and lessens the changes in the dipole moment (Braccini & Perez, 2001), which makes the absorption peak at 2938 cm^{-1} weak. This indicates interactions between NaAlg and Ca^{2+}. When GO was added, the peak at 3200–3700 cm^{-1} (O–H stretching vibration) broadened. This suggests GO interacts with NaAlg through intermolecular hydrogen bonds, so there should be good miscibility between NaAlg and GO.

3.3. SEM images of GO/NaAlg fibers

The GO/NaAlg fibers look and feel smooth and have uniform diameters. But under SEM observation, their surfaces appear rough as shown in Fig. 3 which shows the surfaces and cross sections of the GO/NaAlg fibers with different GO content. Along the direction of the fiber, an ordered striped structure is observed which can be attributed to the roughness of the inner surface of the needle orifice and the shrinking of the gel during drying (Watthanaphanit, Supaphol, Tamura, Tokura, & Rujiravanit, 2008). This phenomenon is more prominent as the GO concentration increases (C1, C2). When GO is added, the viscosity of the NaAlg solution increases and the striped structure is not easily destroyed after the solution leaves the orifice and gelatinizes on contacting the coagulation solution. Therefore, the higher the GO content is, the clearer the striped structure appears on the fiber surface. The graphene nanosheets surrounded by the NaAlg matrix can be faintly seen at high GO content (C2). At the same time, the cross sections of the GO/NaAlg fibers become coarser when GO is added (B3, C3). The magnified image shows that the GO sheets are uniformly distributed in the NaAlg matrix, suggesting good compatibility between NaAlg and GO (B4, C4). NaAlg and GO both contain a large number of oxygen-containing groups such as —COOH groups that can be dissociated into $—COO^{-1}$, so they should have good compatibility.

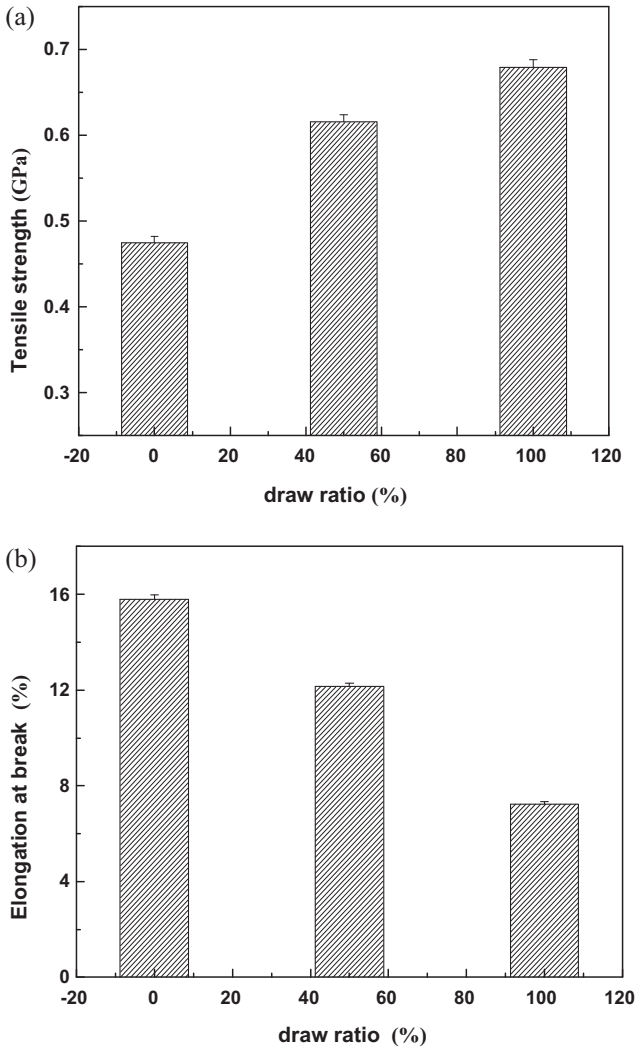

Fig. 7. Tensile strength (a) and elongation at the break (b) of GO/NaAlg fibers with different draw ratios (2 wt% GO).

3.4. Tensile strength and elongation at the break of the GO/NaAlg fibers

Mechanical properties are important parameters in evaluating fibers. The tensile strength and the elongation at the break of both the alginate fiber and the GO/NaAlg fibers were investigated and the results are shown in Fig. 4. The tensile strengths of the GO/NaAlg fibers are obviously higher than those of the pure

alginate fiber. A maximum value of 0.62 GPa was achieved at 4 wt% GO loading. The increase in tensile strength is attributed to the good compatibility between the alginate matrix and the GO fillers owing to the presence of strong interactions between the alginate macromolecules and the GO nanosheets. However, when the GO content was further increased, the tensile strength decreased. The elongation at the break tended to decrease with increasing GO content, and a maximum Young's modulus of 4.30 GPa was achieved at 4 wt% GO loading. These phenomena are common in polymer materials reinforced by inorganic fillers. Sa and Kornev (2009) fabricated NaAlg/SWCNT fibers that had a maximum Young's modulus of 6.38 GPa at 23 wt% SWCNT loading.

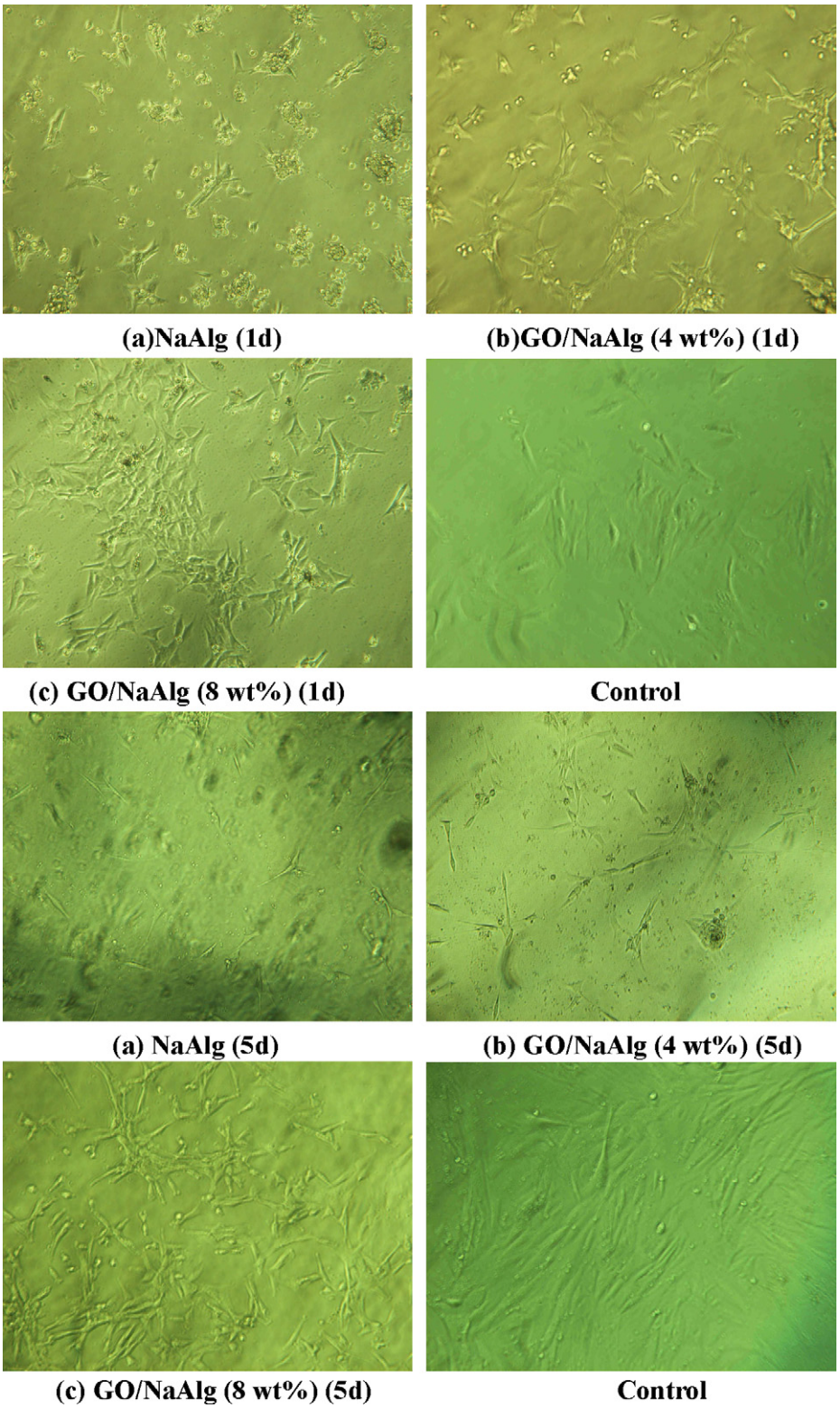

Fig. 8. Microscopic photos of cells cultured on GO/NaAlg fibers in vitro (3×10^4 cells/ml) after 1d, 5d, and 7d (original magnification, ×100).

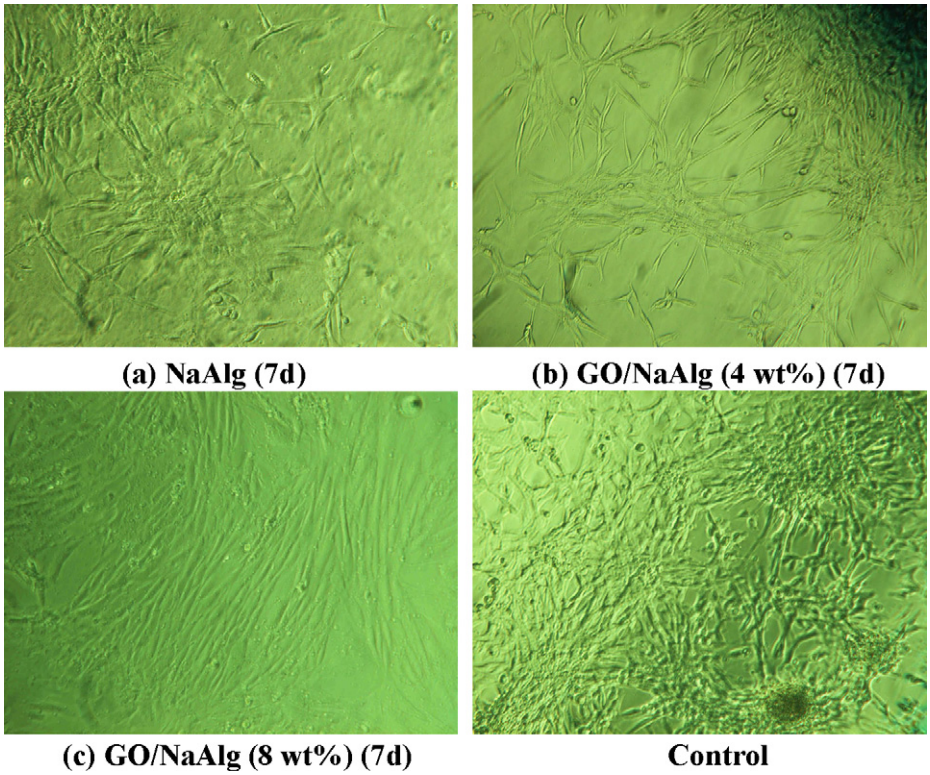

Fig. 8. (*Continued*).

3.5. Water absorbency of GO/NaAlg fibers

Alginate is a natural hydrophilic polymer, so alginate fibers should have a high water absorbency, which is dependent on the composition of the alginate fiber and the properties of the aqueous solution. The water absorbency of different GO/NaAlg fibers in pure water is shown in Fig. 5, and the results indicate that the water absorbency is almost independent of the composition of the GO/NaAlg fibers and is in the range of 0.93–1.06.

3.6. Effects of draw ratio on GO/NaAlg fibers

Fibers have a very large aspect ratio, and uniaxial stretching is often used to improve some properties of the fibers. Here, GO/NaAlg was stretched to obtain hydrogel fibers with 50% and 100% draw ratios and then dried in the stretched state after they went through the coagulation solution. Fig. 6 shows the SEM images of the dried GO/NaAlg fibers with different draw ratios. The stripes on the fiber surface are narrower, deeper and more oriented as the draw ratio is increased. The high magnification images show that the surface of the convex part of the stripes becomes narrower, higher, and appears to have a layered structure (Fig. 6, C3). In the cross section image, the projecting microsheets can only faintly be seen (Fig. 6, C4). They may be oriented graphene sheets formed from the stretching force.

Fig. 7 shows the tensile strength (a) and the elongation at the break (b) of the GO/NaAlg fibers with different draw ratios. The tensile strength increases gradually with increasing draw ratio, whereas the elongation at the break decreases rapidly. Therefore, Young's modulus increases significantly and reaches a maximum value of 9.39 GPa. This can be easily understood if the macromolecule orientation under axially drawing is considered.

3.7. Cell culture

Rabbit's transparent cartilage cells were used as a model cell for seeding and culturing on the GO/NaAlg fibers. During one week of cell culturing, the cells grew well and attached and stretched on the surface of the fibers as shown in Fig. 8. This proves that the GO/NaAlg fibers have good cell affinity and so they are beneficial for cell attachment and growth.

4. Conclusion

NaAlg/GO fibers can be obtained by wet spinning through a $CaCl_2$ coagulating bath. The dry NaAlg/GO fibers look and feel smooth and their diameters can be controlled by adjusting the inner diameter of the needle orifice. NaAlg macromolecules and GO nanosheets both contain a large number of hydrophilic groups such as $-COO^{-1}$, so they have good compatibility which ensures that GO is well dispersed in the NaAlg matrix. Thus, the addition of GO can significantly improve the strength of the NaAlg/GO fibers. When 4 wt% GO is incorporated into the NaAlg fibers, the tensile strengths of the NaAlg/GO fibers increases by 94%, and Young's modulus is 4.3 GPa. For the NaAlg/GO fibers with 2 wt% GO loading, a 100% draw ratio causes Young's modulus to increase from 3.1 to 9.39 GPa. The NaAlg/GO fibers have similar water absorbency to NaAlg fibers in aqueous solution. Since NaAlg/GO fibers are nontoxic, low-cost and high strength, they could have promising applications in biomedical and chemical engineering, environmental protection and other areas.

Acknowledgments

This work was supported by the National Science Foundation of China (21074089, 50873075, 50603017) and Tianjin Municipal

Science and Technology Commission, PR China (09JCZDJC23300). We also thank Dr. Jeanne Wynn for revising the English language.

References

Balakrishnan, B., Mohanty, M., Umashankar, P. R., & Jayakrishnan, A. (2005). Evaluation of an in situ forming hydrogel wound dressing based on oxidized alginate and gelatin. *Biomaterials*, *26*, 6335–6342.

Bogun, M., Mikolajczyk, T., & Rabiej, S. (2009). Effect of formation conditions on the structure and properties of nanocomposite alginate fibers. *Journal of Applied Polymer science*, *114*, 70–82.

Braccini, I., & Perez, S. (2001). Molecular basis of Ca^{2+}-induced gelation in alginates and pectins: The egg-box model revisited. *Biomacromolecules*, *2*, 1089–1096.

Celzard, A., Mcrae, E., Maerche, J. F., Furdin, G., Dufort, M., & Deleuze, C. (1996). Composites based on micron-sized exfoliated graphite particles: Electrical conduction, critical exponents and anisotropy. *Journal of Physics and Chemistry of Solids*, *57*, 715–718.

Chatterjee, S., Lee, M. W., & Woo, S. H. (2009). Enhanced mechanical strength of chitosan hydrogel beads by impregnation with carbon nanotubes. *Carbon*, *47*, 2933–2936.

Chen, H., Muller, M. B., Gilmore, K. J., Wallace, G. G., & Li, D. (2008). Mechanically strong, electrically conductive, and biocompatible graphene paper. *Advanced Materials*, *20*, 3557–3561.

Choi, Y. S., Hong, S. R., Lee, Y. M., Song, K. W., Park, M. H., & Nam, Y. S. (1999). Study on gelatin-containing artificial skin: I. Preparation and characteristics of novel gelatin-alginate sponge. *Biomaterials*, *20*, 409–417.

Chung, T. W., Yang, J., Akaike, T., Cho, K. Y., Nah, J. W., Kim, S. I., et al. (2002). Preparation of alginate/galactosylated chitosan scaffold for hepatocyte attachment. *Biomaterials*, *23*, 2827–2834.

Coleman, J. N., Khan, U., Blau, W. J., & Gun'ko, Y. K. (2006). Small but strong: A review of the mechanical properties of carbon-nanotube-polymer composites. *Carbon*, *44*, 1624–1652.

Dikin, D. A., Stankovich, S., Zimney, E. J., Piner, R. D., Dommett, G. H. B., Evmenenko, G., et al. (2007). Preparation and characterization of graphene oxide paper. *Nature*, *448*, 457–460.

Dong, Z. F., Wang, Q., & Du, Y. M. (2006). Alginate/gelatin blend films and their properties for drug controlled release. *Journal of Membrane Science*, *280*, 37–44.

Feng, L. Z., Zhang, S. A., & Liu, Z. A. (2011). Graphene based gene transfection. *Nanoscale*, *3*, 1252–1257.

Han, D. L., Yan, L. F., Chen, W. F., Li, W., & Bangal, P. R. (2011). Cellulose/graphite oxide composite films with improved mechanical properties over a wide range of temperature. *Carbohydrate Polymers*, *83*, 966–972.

Huang, H., Liu, C. H., Wu, Y., & Fan, S. S. (2005). Aligned carbon nanotube composite films for thermal management. *Advanced Materials*, *17*, 1652–1656.

Hummers, W., & Offeman, R. (1958). Preparation of graphitic oxide. *Journal of the American Chemical Society*, *80*, 1339.

Khan, A., Huq, T., Saha, M., Khan, R. A., & Khan, M. A. (2010). Surface modification of calcium alginate fibers with silane and methyl methacrylate monomers. *Journal of Reinforced Plastics and Composites*, *29*, 3125–3132.

Li, D., & Kaner, R. B. (2008). Graphene-based materials. *Science*, *320*, 1170–1171.

Li, R., Liu, C. H., & Ma, J. (2011). Studies on the properties of graphene oxide-reinforced starch biocomposites. *Carbohydrate Polymers*, *84*, 631–637.

Lu, J. W., Zhu, Y. L., Guo, Z. X., Hu, P., & Yu, J. (2006). Electrospinning of sodium alginate with poly (ethylene oxide). *Polymer*, *47*, 8026–8031.

Meyer, J. C., Geim, A. K., Katsnelson, M. I., Novoselov, K. S., Booth, T. J., & Roth, S. (2007). The structure of suspended graphene sheets. *Nature*, *446*, 60–63.

Paci, J. T., Belytschko, T., & Schatz, G. C. (2007). Computational studies of the structure, behavior upon heating, and mechanical properties of graphite oxide. *Journal of Physical Chemistry C*, *111*, 18099–18111.

Qin, Y. M., Hu, H. Q., & Luo, A. X. (2006). The conversion of calcium alginate fibers into alginic acid fibers and sodium alginate fibers. *Journal of Applied Polymer Science*, *101*, 4216–4221.

Qin, Y. M. (2008). Alginate fibres: An overview of the production processes and applications in wound management. *Polymer International*, *57*, 171–180.

Sennerby, L., Rostlund, T., Albrektsson, B., & Albrektsson, T. (1987). Acute tissue-reactions to potassium alginate with and without color flavor additives. *Biomaterials*, *8*, 49–52.

Speakman, J. B., & Chamberlain, N. H. (1944). The production of rayon from alginic acid. *Journal of the Society of Dyers and Colourists*, *60*, 264–272.

Stankovich, S., Dikin, D. A., Dommett, G. H. B., Kohlhaas, K. M., Zimney, E. J., Stach, E. A., et al. (2006). Graphene-based composite materials. *Nature*, *442*, 282–286.

Sa, V., & Kornev, K. G. (2009). A route toward wet spinning of single walled carbon nanotube fibers: Sodium alginate-SWCNT fibers. Polymer-based smart materials-processes, properties and application. *Materials Research Society Symposium Proceedings*, *1134*, 127–132.

Wang, J. Z., Huang, X. B., Xiao, J., Yu, W. T., Wang, W., Xie, W. Y., et al. (2010). Hydro-spinning: A novel technology for making alginate/chitosan fibrous scaffold. *Journal of Biomedical Materials Research Part*, *93A*, 910–919.

Watthanaphanit, A., Supaphol, P., Tamura, H., Tokura, S., & Rujiravanit, R. (2008). Fabrication, structure, and properties of chitin whisker-reinforced alginate nanocomposite fibers. *Journal of Applied Polymer Science*, *110*, 890–899.

Watthanaphanit, A., Supaphol, P., Tamura, H., Tokura, S., & Rujiravanit, R. (2010). Wet-spun alginate/chitosan whiskers nanocomposite fibers: Preparation, characterization and release characteristic of the whiskers. *Carbohydrate Polymers*, *79*, 738–746.

Woraharn, S., Chaiyasut, C., Sirithunyalug, B., & Sirithunyalug, J. (2010). Survival enhancement of probiotic *Lactobacillus plantarum* CMU-FP002 by granulation and encapsulation techniques. *African Journal of Microbiology Research*, *4*, 2086–2093.

Wu, H., Wan, Y., Cao, X. D., & Wu, Q. (2008). Proliferation of chondrocytes on porous poly(D,L-549 lactide)/chitosan scaffolds. *Acta Biomaterialia*, *4*, 76–87.